Power spectra and variance of laser-noise-induced population fluctuations in two-level atoms

H. Ritsch and P. Zoller
Institut für Theoretische Physik, Universität Innsbruck, 6020 Innsbruck, Austria

J. Cooper
Joint Institute for Laboratory Astrophysics, University of Colorado and National Institute of Standards and Technology, Boulder, Colorado 80309-0440

(Received 27 September 1989)

Variances and power spectra of the resonance fluorescence intensity induced by laser noise in two-level systems are studied theoretically. The effects of amplitude and phase noise fluctuations of a single-mode laser are investigated. Correlations of amplitude and phase fluctuations, as is relevant for excitation with diode lasers, are shown to lead to pronounced asymmetries in variance spectra.

I. INTRODUCTION

The influence of laser noise on the dynamics of atomic systems has been the subject of much theoretical and experimental work in the past decade.[1] So far most of the theoretical work has concentrated on calculating mean values of atomic populations and transition probabilities.[1] However, as we have shown in previous work (Ref. 2, called I in the following; see also Refs. 3 and 4) additional information can be obtained by looking also at the variances of these populations which are particularly sensitive to higher-order statistics of the exciting light field. In this previous work we discussed fluctuations in the resonance fluorescence signal from two- and three-level systems for a phase-diffusing and phase-jumping laser field (with a Lorentzian line shape). A detailed experimental investigation of these effects is presently being performed at the Joint Institute for Laboratory Astrophysics (JILA) using a modulated laser[5] to simulate a phase-diffusing field of variable bandwidths and different line shapes. The experimental results reported are in good agreement with the theoretical predictions.[6]

It is the purpose of the present paper (i) to generalize our previous treatment of population variances in two-level systems to include amplitude fluctuations of a single-mode laser, and (ii) to calculate the power spectra of the intensity fluctuations of the emitted fluorescence. In particular the case of correlated amplitude-phase fluctuations is of interest in the context of excitation with diode lasers[7] [as predicted, for example, by the detuned rotating wave Van der Pol oscillator (DRWVPO) model[7]]. We will show that such correlations lead to asymmetries and shifts in the fluorescence line shape as well as to pronounced asymmetries in variance spectra.[6,8] Additional information on the population noise is contained in power spectra of the intensity fluctuations of the emitted fluorescence. In this paper we discuss, motivated by the JILA experiment,[6] spectra for the phase-diffusion model (PDM) with non-Lorentzian line shape, as well as for the case of amplitude noise.

This paper is organized as follows. In Sec. II we briefly outline the connection between measured intensity fluctuations of the atomic fluorescence and the stochastic expectation values of the atomic density matrix elements. In Sec. III we introduce and discuss stochastic laser models. In Sec. IV we calculate the variance of the upper-state population as a function of laser detuning, while in Sec. V we present results obtained for the power spectra.

II. PHOTODETECTION OF ATOMIC FLUORESCENCE

We consider a large number N of two-level atoms with ground state $|0\rangle$ and upper state $|1\rangle$, which are randomly distributed in a finite interaction region and exposed to a fluctuating laser field with complex amplitude $\mathcal{E}(t)$. The mean distance of the individual atoms is assumed to be much larger than the optical wavelength, while the dimension of the interaction region is taken as being much smaller than the coherence time of the laser light over the velocity of light. Thus we have a sample of many independent atoms exposed to the same fluctuating laser field.

According to Ref. 9 the mean photocurrent of a detector positioned at $\mathbf{x}$ is given by

$$\langle\langle i(t)\rangle\rangle = \eta \int_S dx \langle\langle \langle I_D(\mathbf{x},t)\rangle \rangle\rangle , \tag{2.1}$$

with S the surface of the detector. $I_D(\mathbf{x},t)=\mathbf{E}^-(\mathbf{x},t)\cdot\mathbf{E}^+(\mathbf{x},t)$ is (proportional to) the field intensity operator in the Heisenberg picture at the detector position $\mathbf{x}$ and time t, expressed in terms of the positive [negative] frequency part of the electric field operator $\mathbf{E}^+(\mathbf{x},t)$ [$\mathbf{E}^-(\mathbf{x},t)$]. η is the quantum efficiency of the detector. Following Mollow's treatment of resonance fluorescence[10] the field strength $\mathbf{E}^-(\mathbf{x},t)$ is written as the sum over the contributions of all individual atoms,[10]

$$\begin{aligned}\mathbf{E}^-(\mathbf{x},t) &= \mathbf{E}_f(\mathbf{x},t)+\sum_k \mathbf{E}^{-(k)}(\mathbf{x},t) \\ &= \mathbf{E}_f(\mathbf{x},t)+\sum_k \boldsymbol{\varphi}(\mathbf{x}^k)a^{(k)}(t-|\mathbf{x}-\mathbf{x}^{(k)}|/c) ,\end{aligned} \tag{2.2}$$

with $a^{(k)}$ the lowering operator of the kth atom located at position $\mathbf{x}^{(k)}$ at the retarded time. $\mathbf{E}_f(\mathbf{x},t)$ denotes the vacuum part of the electric field amplitude. φ is a geometrical dipole factor as given in Ref. 10. In Eq. (2.1) $\langle\ \rangle$ denotes the quantum average over the atoms and the vacuum field, while $\langle\langle\ \rangle\rangle$ indicates averaging over the stochastic laser field amplitude $\mathcal{E}(t)$.

Similarly, for the symmetric two-time photocurrent correlation function we have[9]

$$\langle\langle i(t)i(t+\tau)\rangle\rangle = \langle\langle i(t)\rangle\rangle\delta(\tau) + \eta^2\int_S\int_S d\mathbf{x}\,d\mathbf{x}'\langle\langle\langle :I_D(\mathbf{x},t)I_D(\mathbf{x}',t+\tau):\rangle\rangle , \tag{2.3}$$

where :: denotes normal and time ordering. The power spectrum $S(\omega)$ of the intensity fluctuations is defined as the Fourier transform of the stationary two-time current correlation function (2.3),

$$S(\omega)=\int_0^\infty d\tau\cos(\omega\tau)\langle\langle i(0),i(\tau)\rangle\rangle , \tag{2.4}$$

where we adopt the notation $\langle\langle a,b\rangle\rangle=\langle\langle ab\rangle\rangle - \langle\langle a\rangle\rangle\langle\langle b\rangle\rangle$.

The first term on the right-hand side of Eq. (2.3) is the shot-noise contribution which gives a flat background in the spectrum (2.4). This term is negligible for a large number of atoms N, since it scales proportional with N while the second term in Eq. (2.3) goes with N^2 (see the discussion below). Following Ref. 11 the second term in Eq. (2.3) can be expressed as

$$\eta^2\int_S\int_S d\mathbf{x}\,d\mathbf{x}'\left[\sum_k\sum_{l\atop k\neq l}[\langle\langle\langle E^{-(k)}(\mathbf{x},t)E^{+(k)}(\mathbf{x}',t+\tau)E^{-(l)}(\mathbf{x},t)E^{+(l)}(\mathbf{x}',t+\tau)\rangle\rangle\rangle + \langle\langle\langle E^{-(k)}(\mathbf{x},t)E^{-(l)}(\mathbf{x}',t+\tau)E^{+(l)}(\mathbf{x}',t+\tau)E^{+(k)}(\mathbf{x},t)\rangle\rangle\rangle] + \sum_k\langle\langle\langle E^{-(k)}(\mathbf{x},t)E^{-(k)}(\mathbf{x}',t+\tau)E^{+(k)}(\mathbf{x},t+\tau)E^{+(k)}(\mathbf{x}',t)\rangle\rangle\rangle\right] \tag{2.5}$$

(for simplicity of writing we have ignored the vector character of the electric field). In Eq. (2.5) the second term is the dominant contribution. This is valid for a large number of atoms and a detector area which is much larger than the coherence area; in addition antibunching (which is a single-atom effect) is ignored. Assuming the atoms to be independent, we can take the quantum average for each atom separately, so that we get

$$\langle\langle i(t)i(t+\tau)\rangle\rangle = \eta^2\int_S\int_S d\mathbf{x}\,d\mathbf{x}'\sum_k\sum_{l\atop k\neq l}\langle\langle\langle I^{(k)}(x,t)\rangle\times\langle I^{(l)}(x',t+\tau)\rangle\rangle\rangle , \tag{2.6}$$

where $\langle I^{(k)}\rangle$ is the intensity contribution from the kth atom,

$$\langle I^{(k)}(\mathbf{x},t)\rangle=\kappa\frac{\Omega_a}{4\pi}\rho_{11}^{(k)}(t-|\mathbf{x}-\mathbf{x}^{(k)}|/c) , \tag{2.7}$$

where κ is the atomic decay rate and the solid angle Ω_a accounts for the portion of the emitted fluorescence energy that is collected by the detection optics. $\rho_{11}^{(k)}(t)$ is the expectation value of the atomic upper-state (from which the fluorescence is detected) population of the kth atom.

If we assume that the dimension of the sample is small compared to the fluctuation time of the signal times the velocity of light, we find[12]

$$\langle\langle i(t)i(t+\tau)\rangle\rangle = (\eta\kappa\Omega/4\pi)^2\sum_k\sum_{l\atop k\neq l}\langle\langle\rho_{11}^{(k)}(t)\rho_{11}^{(l)}(t+\tau)\rangle\rangle . \tag{2.8}$$

In general $\rho_{11}^{(k)}$ for an atom at position $\mathbf{x}^{(k)}$ depends on the field $\mathbf{E}(\mathbf{x}^{(k)},t)$ at this position as well as the velocity $\mathbf{v}^{(k)}(t)$. However, in this paper we will ignore the spatial intensity distribution of the laser and the Doppler shifts of the individual atoms. This allows us to drop the atomic labels k and l in Eq. (2.8) with the result

$$\langle\langle i(t)i(t+\tau)\rangle\rangle=(\eta\kappa\Omega/4\pi)^2N(N-1)\times\langle\langle\rho_{11}(t)\rho_{11}(t+\tau)\rangle\rangle . \tag{2.9}$$

The preceding discussion relates the variance of the intensity fluctuations of the resonance fluorescence signal of an ensemble of atoms to the stochastic averages of the expectation value of the atomic upper-state population of the two-level system $\langle\langle\rho_{11}(t)\rangle\rangle$ and its autocorrelation function $\langle\langle\rho_{11}(t+\tau),\rho_{11}(t)\rangle\rangle$. $\rho_{11}(t)$ is a solution of the optical Bloch equations

$$\left[\frac{d}{dt}+\begin{bmatrix} -i\delta+\kappa/2-i\dot{\varphi}(t) & 0 & \frac{i}{2}\Omega(t) \\ 0 & i\delta+\kappa/2+i\dot{\varphi}(t) & -\frac{i}{2}\Omega(t) \\ i\Omega(t) & -i\Omega(t) & \kappa \end{bmatrix}\right]\begin{bmatrix}\rho_{10}\\ \rho_{01}\\ w\end{bmatrix}=\begin{bmatrix}0\\0\\-\kappa\end{bmatrix} . \tag{2.10}$$

Here $w=\rho_{11}-\rho_{00}$ is the population inversion, ρ_{10} and ρ_{01} are the atomic coherences. $\Omega(t)=2\mu\epsilon|\mathcal{E}(t)|$ is the Rabi frequency with μ the atomic dipole matrix element, ϵ the polarization vector of the light, and $\mathcal{E}(t)=|\mathcal{E}(t)|e^{-i\varphi(t)}$ the complex laser amplitude with $\varphi(t)$ the laser phase; δ is the detuning from the atomic transition frequency.[13] Equations for the population variance

$$\Delta\rho_{11}^2=\langle\langle(\rho_{11}-\langle\langle\rho_{11}\rangle\rangle)^2\rangle\rangle=\tfrac{1}{4}(\langle\langle w^2\rangle\rangle-\langle\langle w\rangle\rangle^2)$$

can be derived by introducing a vector of squared density matrix elements

$$\left[\frac{d}{dt}+\begin{bmatrix} \kappa-i\delta+2i\dot{\varphi} & 0 & 0 & i\Omega & 0 & 0 \\ 0 & \kappa+i\delta-2i\dot{\varphi} & 0 & 0 & -i\Omega & 0 \\ 0 & 0 & \kappa & -i\frac{1}{2}\Omega & i\frac{1}{2}\Omega & 0 \\ i\Omega & 0 & -i\Omega & \frac{3}{2}\kappa-i\delta+i\dot{\varphi} & 0 & i\frac{1}{2}\Omega \\ 0 & -i\Omega & i\Omega & 0 & \frac{3}{2}\kappa+i\delta-i\dot{\varphi} & -i\frac{1}{2}\Omega \\ 0 & 0 & 0 & 2i\Omega & -2i\Omega & 2\kappa \end{bmatrix}\right]\begin{bmatrix} \rho_{10}^2 \\ \rho_{01}^2 \\ \rho_{10}\rho_{01} \\ \rho_{10}w \\ \rho_{01}w \\ w^2 \end{bmatrix}=-\kappa\begin{bmatrix} 0 \\ 0 \\ 0 \\ \rho_{10} \\ \rho_{01} \\ 2w \end{bmatrix}, \tag{2.11}$$

where for simplicity we have suppressed the time argument of Ω and φ. Eqs. (2.10) and (2.11) constitute sets of multiplicative stochastic differential equations which have to be solved for the averages given a stochastic light model $\mathcal{E}(t)$.

III. LASER-NOISE MODELS

We consider two models of stochastic light fluctuations. First we discuss amplitude and phase fluctuation of a single-mode laser, where the case of correlated amplitude-phase fluctuations is of interest in the context of diode lasers. The model employed is a linearized version of the detuned rotating wave Van der Pol oscillator.[7] The second light model is the phase-diffusion model with a non-Lorentzian line shape.[14] This is a generalization of the PDM considered in I, and differs from the standard PDM by relaxing the assumption of an infinitely short frequency correlation time; this leads to a (more realistic) Gaussian cutoff of the (Lorentzian) laser line shape at high frequencies.

A. Detuned rotating wave Van der Pol oscillator

Amplitude and phase fluctuations of a single-mode laser can be modeled by a DRWVPO. The stochastic Ito equations[15] for the complex field amplitude in this case are[7]

$$d\mathcal{E}=-\tfrac{1}{2}\beta_l(E_0^2-|\mathcal{E}|^2)(1+i\alpha)\mathcal{E}\,dt+dF(t)\ . \tag{3.1}$$

The parameter E_0 corresponds to the steady-state amplitude when the noise forces are neglected (we choose E_0 real and positive). The quantity β_l describes the differential gain near the steady-state amplitude and α is the (dimensionless) detuning of the cavity resonance frequency from the active optical transition in units of the cavity linewidth. $dF(t)$ is a complex white-noise increment with $dF^*(t)dF(t')=R\,dt$ where R is the spontaneous emission rate responsible for the laser noise. To characterize the regime of operation of the laser it proves useful to introduce a pump parameter $a_0=\sqrt{2\beta_l/R}\,E_0^2$, with $a_0=0$ characterizing the laser threshold. In writing Eq. (3.1) as well as in this section we adopt the standard conventions of laser theory to normalize the square of the electric field strengths in units of photon numbers.

Far above threshold this model reduces to the PDM of the laser.[7] Via the detuning parameter α this model also includes a coupling of amplitude and phase fluctuations; such correlations are predicted for the output of diode lasers.[7] Here physically, this correlation arises because the fluctuations of the diode laser intensity are accompanied by a change of the refractive index of the active medium which leads to additional phase noise.

Introducing polar coordinates $\mathcal{E}(t)=E(t)e^{-i\varphi(t)}$ and linearizing the laser amplitude around the steady state $E(t)=E_0+e(t)$ assuming $e(t)$ to be a small perturbation ($a_0\gg1$), we derive

$$\begin{aligned} de(t)&=-\lambda e(t)dt+(2\lambda\langle\langle e^2\rangle\rangle)^{1/2}dW_1(t)\ , \\ d\varphi(t)&=-\alpha\lambda e(t)/E_0dt+\sqrt{2b}\,dW_2(t)\ . \end{aligned} \tag{3.2}$$

Here $\lambda=\beta E_0^2$ is the time constant of the intensity fluctuations, $\langle\langle e^2\rangle\rangle=R/4\lambda$ is the variance of the intensity, and $b=\frac{1}{4}R/E_0^2$ can be identified with the bandwidth of the laser when the intensity fluctuations are neglected. $dW_1(t)$ and $dW_2(t)$ are Wiener noise increments.[7(c)] Note the scaling $\lambda\propto a_0$, $b\propto1/a_0$, and $\langle\langle e^2\rangle\rangle/E_0^2=1/(2a_0^2)$ with the pump parameter.

For large pump parameter the amplitude fluctuations become very fast and small. Thus we end up with a pure phase noise model, which reduces to a standard PDM for vanishing coupling parameter $\alpha=0$. For $\alpha\neq0$ the amplitude-induced phase fluctuations, however, cannot be neglected even far above threshold: adiabatically eliminating the amplitude $e(t)$, i.e., assuming the time scale of the amplitude fluctuations to be fast, one finds using the identity $\lambda\langle\langle e^2\rangle\rangle/E_0^2=b$ the phase-diffusion equation

$$d\varphi(t)=[2b(1+\alpha^2)]^{1/2}dW(t) \tag{3.3}$$

with enhanced rate $b_1=b(1+\alpha^2)$.[7(a),7(b)] Operating the laser closer to threshold ($a_0\approx1-3$) the amplitude fluctuations get larger and slower and the correlations between amplitude and phase noise become important. While

these correlations lead to only minor changes in the laser spectrum[7] they still can have a significant effect on the atomic noise spectra (see Secs. IV and V). This provides a tool for a precise investigation of such correlations. Finally, in the case of $\alpha=0$ the amplitude noise is independent of the phase noise. Near laser threshold amplitude fluctuations then constitute the dominant noise contribution.

B. Phase-diffusion model with non-Lorentzian line shape

The PDM with non-Lorentzian line shape is defined by the set of Langevin equations

$$d\varphi(t)=\nu(t)dt,\quad d\nu(t)=-\beta\nu(t)dt+\sqrt{2b}\,\beta\,dW(t)\ . \tag{3.4}$$

For $\beta\gg b$ the laser spectrum predicted by (3.4) resembles a Lorentzian shape at line center with a Gaussian cutoff at β. For $\beta\to\infty$ keeping b fixed this model goes over into the standard PDM (with Lorentzian line shape with bandwidth b),

$$d\varphi(t)=\sqrt{2b}\ dW(t)\ , \tag{3.5}$$

which is the noise model discussed in I.

IV. MEAN VALUES AND VARIANCES OF ATOMIC POPULATIONS

In this section we discuss mean values and variances of atomic populations for the noise models of Sec. III. We have collected some of the formal and technical steps of averaging the optical Bloch equations over the laser noise in Appendix A.

A. Detuned rotating wave Van der Pol oscillator

The optical Bloch equations (2.10) have the form

$$d\mathbf{u}(t)+[\underline{A}+\Omega'(t)\underline{B}_1]\mathbf{u}(t)\,dt+d\varphi(t)\underline{B}_2\mathbf{u}(t)+\mathbf{I}\,dt=0 \tag{4.1}$$

with $\mathbf{u}(t)$ a vector of density matrix elements and $\underline{A}$, $\underline{B}_1$, and $\underline{B}_2$ matrices and $\mathbf{I}$ a constant vector which are readily read off from (2.10). $\Omega'(t)=2\mu\epsilon|e(t)|$ and $\varphi(t)$ are the stochastic Rabi frequency and phase, respectively, obeying the Langevin equations [compare Eq. (3.2)]

$$\begin{aligned} d\Omega'(t)&=-\lambda\Omega'(t)dt+(2\lambda\langle\langle\Omega'^2\rangle\rangle)^{1/2}dW_1(t)\ ,\\ d\varphi(t)&=-\alpha\lambda\Omega'(t)/\Omega_0dt+\sqrt{2b}\,dW_2(t)\ . \end{aligned} \tag{4.2}$$

Inserting the phase equation into the Eq. (4.1) it is easy to perform the averaging over the noise force $dW_2(t)$ which leads to

$$d\langle\langle\mathbf{u}(t)\rangle\rangle_2+\{\underline{A}+\Omega'(t)[\underline{B}_1-(\alpha\lambda/\Omega_0)\underline{B}_2]-b\underline{B}_2^2\}\langle\langle\mathbf{u}(t)\rangle\rangle_2dt+\mathbf{I}\,dt=0\ . \tag{4.3}$$

Here $b\underline{B}_2^2$ is the usual phase-diffusion damping term. Note the appearance of the term $\Omega'(t)(\alpha\lambda/\Omega_0)\underline{B}_2$ which describes the effect of phase fluctuations correlated with amplitude noise. As outlined in Appendix A for arbitrary correlation time λ the stationary averages $\langle\langle\mathbf{u}(t)\rangle\rangle$ can be obtained from a matrix continued fraction expansion.

Before presenting the results obtained from numerical calculations, we will discuss the basic structure of the equations in the limit of fast amplitude fluctuations, i.e., when λ is much faster than all of the other time scales in the problem. In this limit we can truncate the matrix continued fraction expansion in lowest nontrivial order. For the stationary atomic density matrix elements we find

$$\frac{d}{dt}\langle\langle\mathbf{u}(t)\rangle\rangle+[\underline{A}-(\langle\langle\Omega'^2\rangle\rangle/\lambda)\underline{B}_1^2-(\alpha\langle\langle\Omega'^2\rangle\rangle/\Omega_0)(\underline{B}_1\underline{B}_2+\underline{B}_2\underline{B}_1)-b_1\underline{B}_2^2]\langle\langle\mathbf{u}(t)\rangle\rangle+\mathbf{I}=0\ , \tag{4.4a}$$

or explicitly

$$\left[\frac{d}{dt}+\begin{bmatrix} -i\delta+\kappa/2+n & -n & \frac{i}{2}\tilde{\Omega}^* \\ -n & i\delta+\kappa/2+n & -\frac{i}{2}\tilde{\Omega} \\ i\tilde{\Omega}^* & -i\tilde{\Omega} & \kappa \end{bmatrix}\right]\begin{bmatrix}\langle\langle\rho_{10}\rangle\rangle\\ \langle\langle\rho_{01}\rangle\rangle\\ \langle\langle w\rangle\rangle\end{bmatrix}=\begin{bmatrix}0\\0\\-\kappa\end{bmatrix}\ . \tag{4.4b}$$

Here $n=\langle\langle\Omega'^2\rangle\rangle/2\lambda$ is an amplitude-noise-induced transition rate between the atomic levels which appears as additional damping terms for the atomic coherences and population inversion. As expected from the considerations in Sec. III, far above threshold ($a_0\gg1$) n becomes negligible and the equations reduce to the case treated in our earlier work. Note, however, that the effective phase-diffusion rate $b_1=(1+\alpha^2)b$ is enhanced by an amount a^2b stemming from the amplitude-induced phase noise. The relative size of the contributions in the sum is

independent of laser intensity and only depends on α. Typical values for α in some diode lasers are of the order $\alpha \approx 1-5$, so that the amplitude-induced phase noise can be the dominant term. An interesting feature of the Bloch equations (4.4) is the appearance of a complex Rabi frequency $\tilde{\Omega}=\Omega_0 - i\langle\langle \Omega'^2 \rangle\rangle/\Omega_0$, which is responsible for an asymmetry of the upper-state population as a function of laser detuning. For the stationary mean value of the atomic inversion we find

$$\langle\langle w \rangle\rangle = -\left[1+\frac{2n}{\kappa}+\frac{\Omega_0^2\kappa_p+2\langle\langle \Omega'^2\rangle\rangle\left[\alpha\delta-\alpha^2\frac{\langle\langle \Omega'^2\rangle\rangle}{\Omega_0^2}(\kappa_p+n)\right]}{\kappa(\kappa_p^2+2\kappa_p n+\delta^2)}\right]^{-1}, \tag{4.5}$$

with $\kappa_p=\frac{1}{2}\kappa+b(1+\alpha^2)$. It is the term proportional to $\alpha\delta$, stemming from the correlation between amplitude and phase fluctuations, which introduces an asymmetry in the upper-state population as a function of laser detuning. As we will see below this effect is even more drastic for the atomic population variances.

The behavior of the variances can be discussed in an analogous way: arranging the squares of the density matrix elements in a vector $\mathbf{U}$ as in (2.11) one finds an equation of the form

$$d\mathbf{U}(t)+[\mathcal{A}+\Omega'(t)\mathcal{B}_1]\mathbf{U}(t)dt + d\varphi(t)\underline{\mathcal{B}}_2\mathbf{U}(t)+\underline{\mathcal{C}}\mathbf{u}(t)dt=\mathbf{0}\ , \tag{4.6}$$

where again the matrices $\underline{\mathcal{A}}$, $\underline{\mathcal{B}}_1$, $\underline{\mathcal{B}}_2$, and $\underline{\mathcal{C}}$ can be immediately read off from (2.11). As outlined in Appendix A solution of (4.6) for the stationary averages of $\mathbf{U}(t)$ parallels the discussion given above for Eq. (4.1)

In the following we will illustrate some of the results obtained by numerical evaluation of the matrix continued fraction (see Appendix A) for the DRWVPO model up to the necessary order of truncation to achieve convergence. As a first step we will confine ourselves to the case of independent amplitude and phase fluctuations, i.e., $\alpha=0$. In Fig. 1 we plot the stationary variance of the upper-state population as a function of laser detuning for $b=0.25\kappa$, $\Omega_0=0.25\kappa$, $\lambda=2\kappa$, and decreasing amplitude noise $n/\Omega_0=0.05$ (solid line), $n/\Omega_0=0.01$ (dashed line), and $n/\Omega_0=5\times10^{-5}$ (dotted line). For small amplitude fluctuations we find a clearly visible dip at line center (as in the case of the PDM in I) which is destroyed succes-

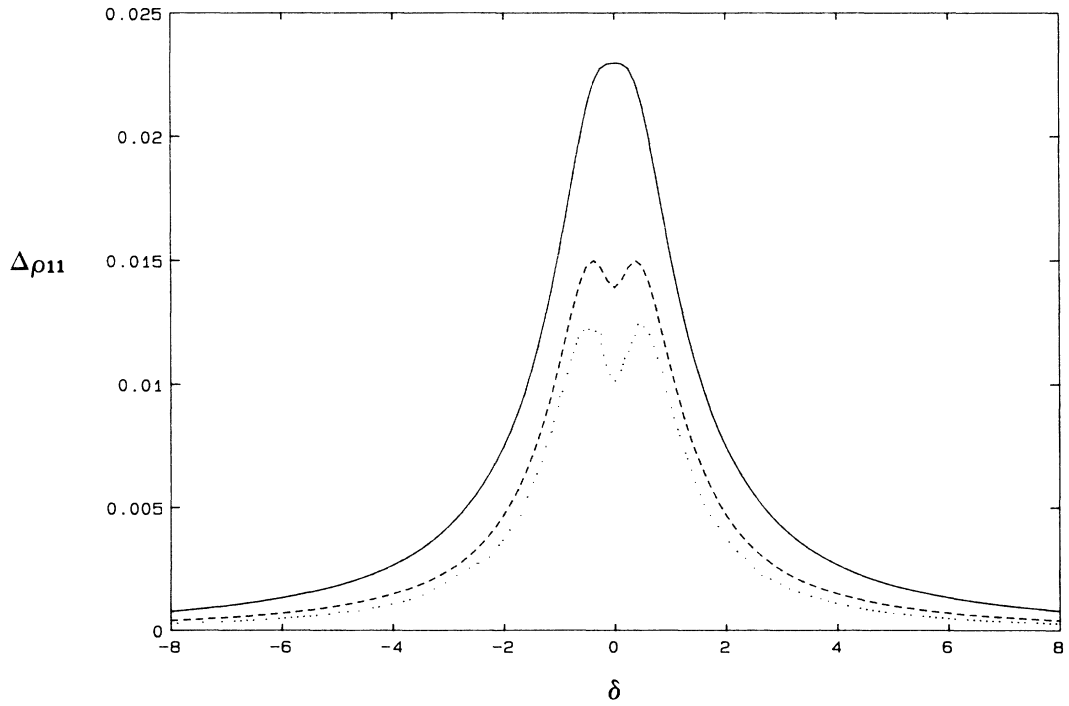

FIG. 1. Variance of the upper-state population fluctuations $\Delta\rho_{11}$ as a function of laser detuning δ for the linearized RWVPO model with $b=0.25\kappa$, $\Omega_0=0.25\kappa$, $\alpha=0$, and $\lambda=2\kappa$. The different curves correspond to $n/\Omega_0=0.15$ (solid line), $n/\Omega_0=0.01$ (dashed line), and $n/\Omega_0=5\times10^{-5}$ (dotted line).

sively by an increasing amount of amplitude noise. Because the maximum of the amplitude-induced noise just coincides with the minimum of the phase-diffusion-induced noise at $\delta=0$, even small amounts of amplitude noise can produce an easily visible effect.

Let us now come to the case $\alpha\neq 0$. In Fig. 2(a) we show the mean upper-state population as a function of laser detuning δ/κ for a coupling constant $\alpha=3$, noise

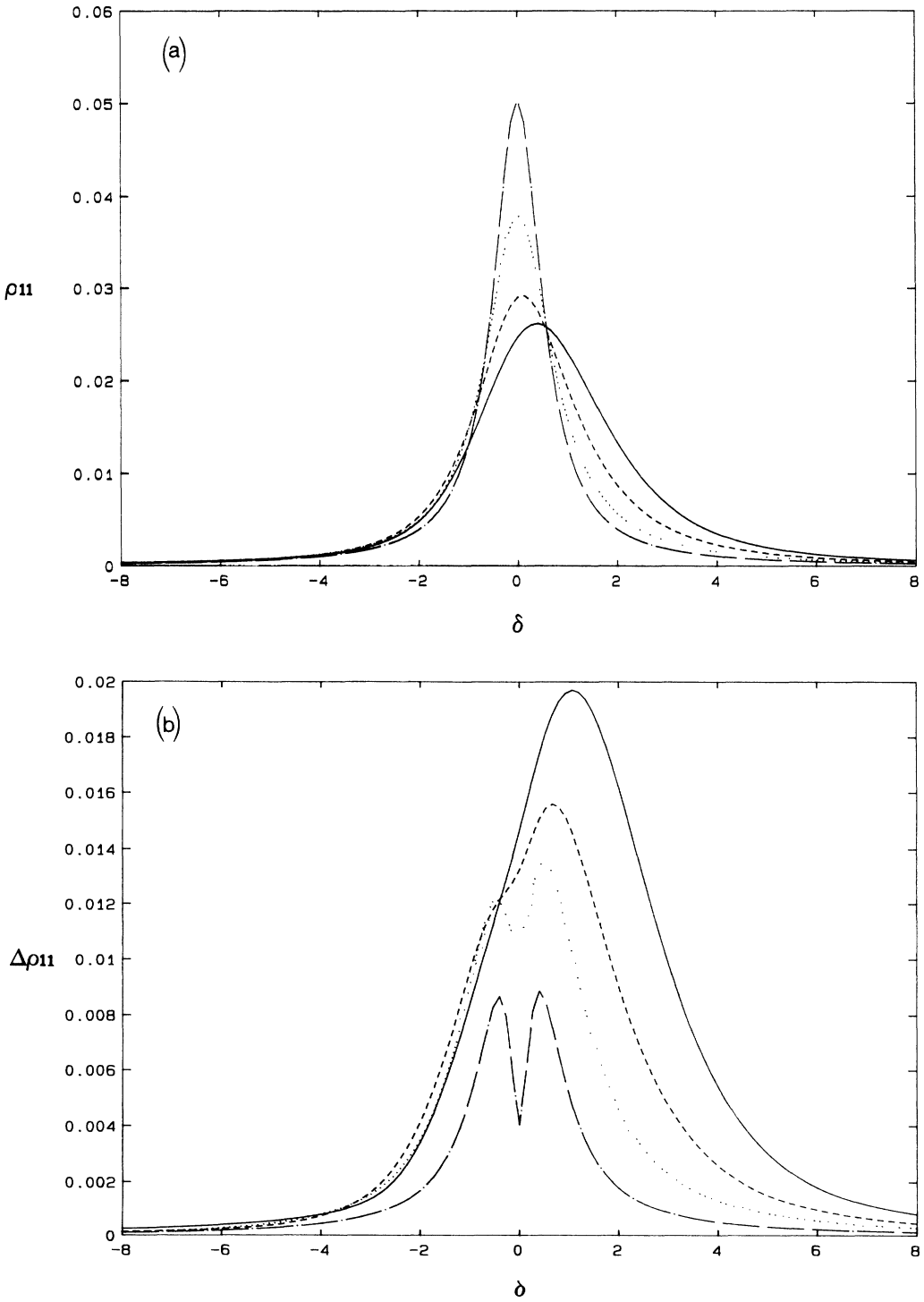

FIG. 2. Mean population $\langle\langle \rho_{11} \rangle\rangle$ (a) and variance $\Delta\rho_{11}$ (b) as a function of laser detuning δ for the linearized DRWVPO model, with $\alpha=3$, $R=\kappa/3$, $\Omega_0=0.25\kappa$, and $\beta=2\kappa$. The parameters for the various curves are $a_0=1$ (solid line), $a_0=2$ (dashed line), $a_0=5$ (dotted line), and $a_0=25$ (dash-dotted line).

strength $R=\kappa/3$, $\beta_l=2\kappa$, and four increasing values of the pump parameter $a_0=1$ (solid line), $a_0=2$ (dashed line), $a_0=5$ (dotted line), and $a_0=25$ (dash-dotted line); note that these parameters are associated with parameter values $\lambda=a_0/\sqrt{3}\kappa$. In order to separate the effect due to differing noise properties from saturation effects, we have chosen the atom field coupling so that the Rabi frequency $\Omega_0=0.25\kappa$ is the same for all four curves. One clearly sees a broadening of the line with decreasing pump parameter, which is accompanied by a shift of the line from

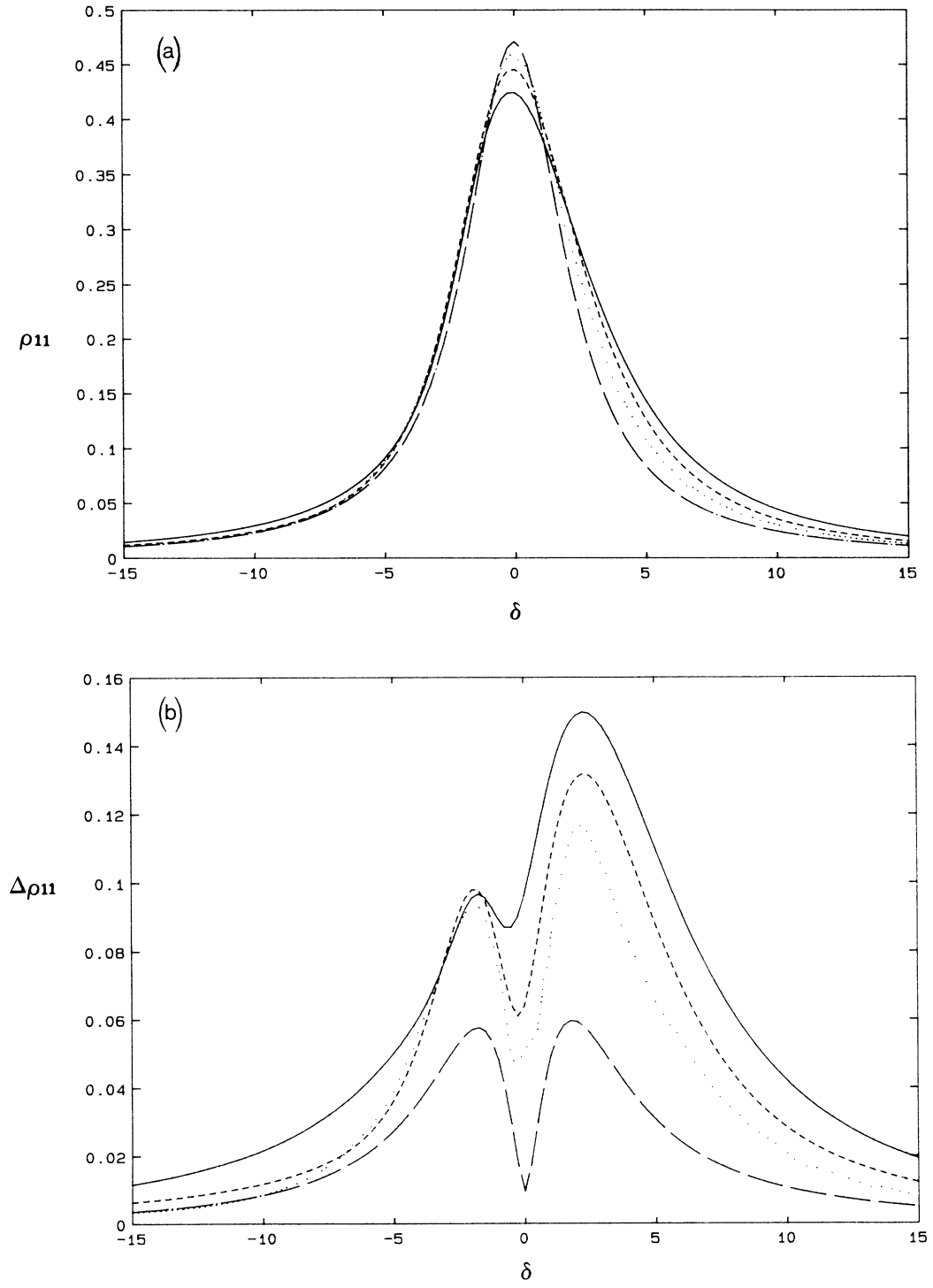

FIG. 3. Same as Fig. 2 with $\Omega_0=3\kappa$.

resonance and a slight asymmetry. Qualitatively this stems from the fact that a fluctuation towards higher intensity is always accompanied by a rapid phase change (frequency shift), so that, depending on the sign of α, higher or lower frequency components in the laser output are more pronounced.

A much more dramatic change can be seen in the variance spectra. We demonstrate this in Fig. 2(b), where we

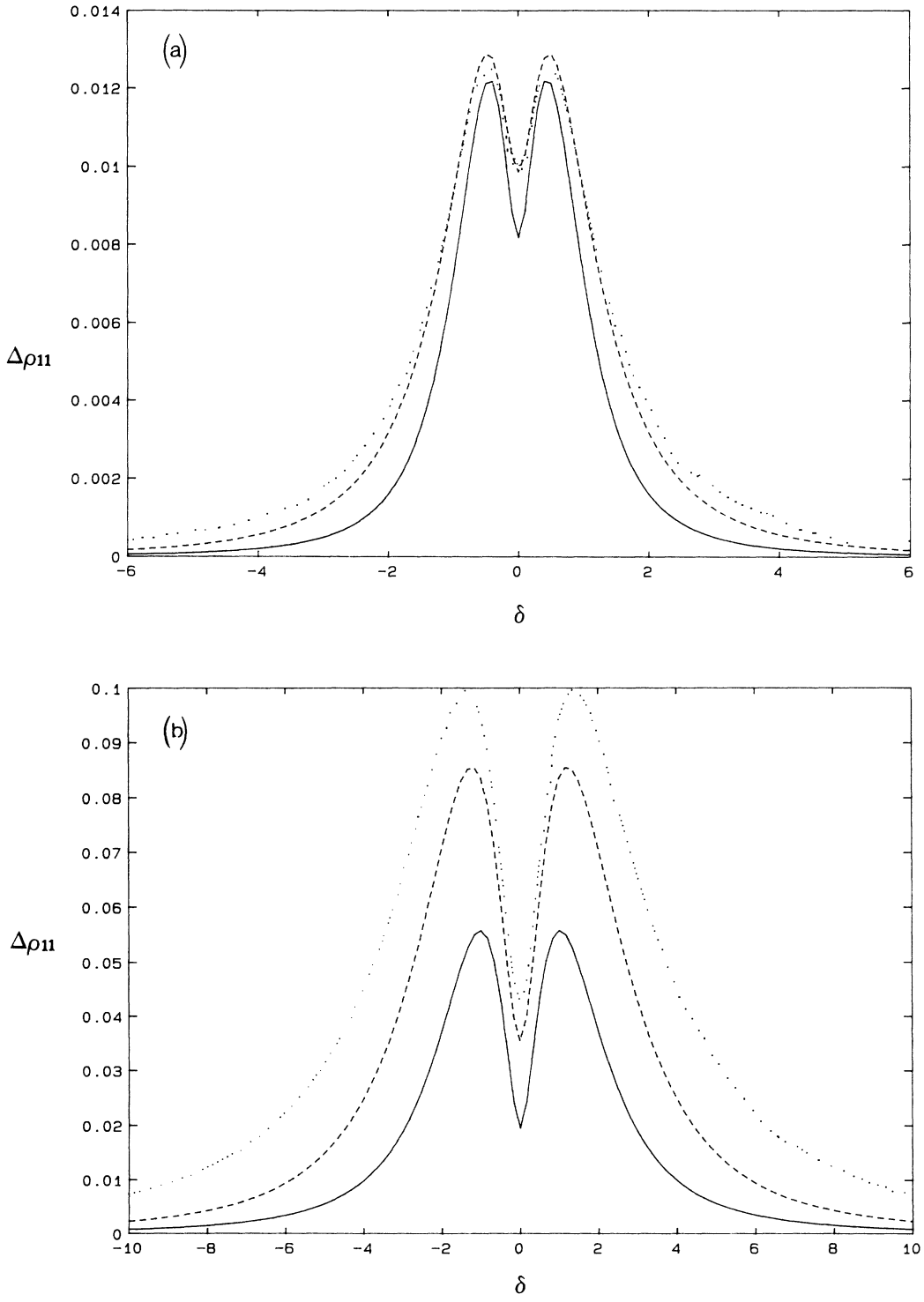

FIG. 4. Variance of the upper-state population fluctuations $\Delta\rho_{11}$ as a function of laser detuning δ for the PDM with non-Lorentzian line shape with $b=0.25\kappa$, $\Omega_0=0.25\kappa$, (a) and $\Omega_0=2\kappa$ (b). The different curves correspond to $\beta=0.5\kappa$ (solid line), $\beta=2\kappa$ (dashed line), and $\beta=10\kappa$ (dotted line).

plot the stationary upper-state variance $\Delta\rho_{11}$ as a function of laser detuning δ for the same parameters as above. As expected, with decreasing pump parameter the noise increases. Additionally we get an increasing asymmetry between the two "phase diffusion" maxima, which near threshold gets so large that only one peak remains visible. Note that the asymmetry for the dashed and the dotted line is clearly visible in the variance spectra, while it can hardly be seen in the curves for the mean population.

As might be expected from Eq. (4.5) the asymmetries are even more enhanced for larger Rabi frequencies. We show this in Figs. 3(a) and 3(b), where we plot $\langle\langle\rho_{11}\rangle\rangle$ and $\Delta\rho_{11}$ as a function of laser detuning δ for $\Omega_0=3\kappa$. The other parameters are chosen as in Fig. 2. Note that the curves for the mean population are all very similar, whereas there is a pronounced asymmetry in the variance spectra. Hence the latter provide a much more sensitive tool for detecting amplitude-phase noise correlations than analyzing mean values alone.

B. Phase-diffusion model with non-Lorentzian line shape

Here again the optical Bloch equations can be written in the form

$$d\mathbf{u}(t)+[\underline{A}+\nu(t)\underline{B}]\mathbf{u}(t)dt+\mathbf{I}\,dt=0 \tag{4.7}$$

with $\nu(t)$ an Ornstein-Uhlenbeck process obeying Eq. (3.4). The solution of Eq. (4.7) can again be obtained by matrix continued fraction techniques outlined in Appendix A. In the limit when β is larger than all other time scales a lowest-order truncation of the continued fraction is sufficient and the results reduce to those obtained in I. Below we concentrate on finite-β effects.

In Figs. 4(a) and 4(b) we show $\Delta\rho_{11}$ as a function of δ for three different values of β: $\beta=10\kappa$ (dotted line, corresponding to the fast fluctuation limit), $\beta=2\kappa$ (dashed line), and $\beta=0.5\kappa$ (solid line) and $b=0.25\kappa$. For small Rabi frequency $\Omega_0=\frac{1}{4}\kappa$ we see that with decreasing cutoff frequency β mainly the noise in the wings is decreased, while the two maxima near line center are even slightly enhanced so that the dip at $\delta=0$ even becomes more pronounced. From this one might conclude that the high frequency part of the noise is responsible for the upper-state variance at large detunings, although there is not a direct one-to-one correspondence. For finite β the signal-to-noise ratio $\Delta\rho_{11}/\rho_{11}$ stays below unity in the limit of large detunings. For a larger Rabi frequency $\Omega_0=2\kappa$ [Fig. 4(b)] we find a much stronger dependence of the noise intensity on β, which gets efficiently quenched with decreasing β for all values of δ (although again the wings get apparently more quenched).

V. POWER SPECTRA OF FLUORESCENCE INTENSITY FLUCTUATIONS

As we have shown in Sec. II the power spectrum of the fluorescence intensity fluctuations is proportional to the Fourier transform of the stationary autocorrelation function of the upper-state population, which we normalize here according to

$$S(\omega)=\int_0^\infty d\tau\cos(\omega\tau)\langle\langle\rho_{11}(t+\tau),\rho_{11}(t)\rangle\rangle\ . \tag{5.1}$$

Obviously, $S(\omega)$ is symmetric in ω and we have $2/\pi\int_0^\infty d\omega\,S(\omega)=\Delta\rho_{11}^2$.

A. Phase-diffusion model

Simple analytical results can be obtained for the PDM with Lorentzian line shape and bandwidth $b(\beta\to\infty)$. According to Eq. (B3) in Appendix B, the power spectrum (5.1) is

$$S(\omega)=\tfrac{1}{4}\mathrm{Re}\left[\frac{\langle\langle w,w\rangle\rangle-i\Omega\langle\langle\rho_{10},w\rangle\rangle/(i\omega+z^*)+i\Omega\langle\langle\rho_{01},w\rangle\rangle/(i\omega+z)}{i\omega+\kappa+\frac{1}{2}\Omega^2/(i\omega+z^*)+\frac{1}{2}\Omega^2/(i\omega+z)}\right], \tag{5.2}$$

where $z=i\delta+\frac{1}{2}\kappa+b$ and the variances of the density matrix elements are known from I. Note that the denominator in Eq. (5.2) has three roots as a function of ω (which, of course, are related to characteristic frequencies in the time evolution of the density matrix).

In the general case of the PDM with non-Lorentzian line shape the spectrum can be calculated from a matrix continued fraction expansion developed in Appendix A. In Figs. 5(a)–5(d) we show $S(\omega)$ as a function of frequency ω. In each of these figures the three curves correspond to frequency correlation times $\beta=2\kappa$ (solid line), $\beta=5.5\kappa$ (dashed line), and $\beta=9\kappa$ (dotted line, corresponding closely to the Lorentzian limit). For zero detuning $\delta=0$ and small Rabi frequency $\Omega=0.25\kappa$ [Fig. 5(a)] we have only a weak dependence on the frequency correlation time and all curves show a similar behavior with a single maximum centered around zero frequency. Increasing the laser detuning $\delta=3\kappa$ [Fig. 5(b)] this simple behavior is changed and we find a double peaked structure with a larger peak at $\omega=\delta$ and a smaller maximum at $\omega=0$. In this case we also get a strong dependence on the frequency correlation time β; for small β the noise decreases rapidly for $\omega>\delta$ and the peak at zero frequency gets suppressed. For a larger Rabi frequency $\Omega=2.5\kappa$ and small detuning $\delta=0$ [Fig. 5(c)] we still find a single peak, but it is now shifted to $\omega=\Omega$ and gets larger with growing β. For a larger detuning again we get a doubly peaked structure, where the relative magnitude of the two peaks strongly depends on β. This can be clearly seen in Fig. 5(d), where we have set $\Omega=2.5\kappa$ and the detuning is $\delta=2\kappa$. For small $\beta\approx\kappa$ we find the maximum of the fluctuations at line center, while for large $\beta\gg\kappa$ the fluctuations at high frequencies are strongly increased, so that the second peak gets larger than the center maximum. Overall the tendency is to reduce the spectrum at high ω the most.

B. Amplitude fluctuations

A simple approach to calculate power spectra $S(\omega)$, even though it is somewhat restricted in its validity, is to linearize the atomic equations around their (noise free) steady-state values. This has the advantage of leading to analytical closed-form expression which is valid in the small noise limit. Here we illustrate this technique for

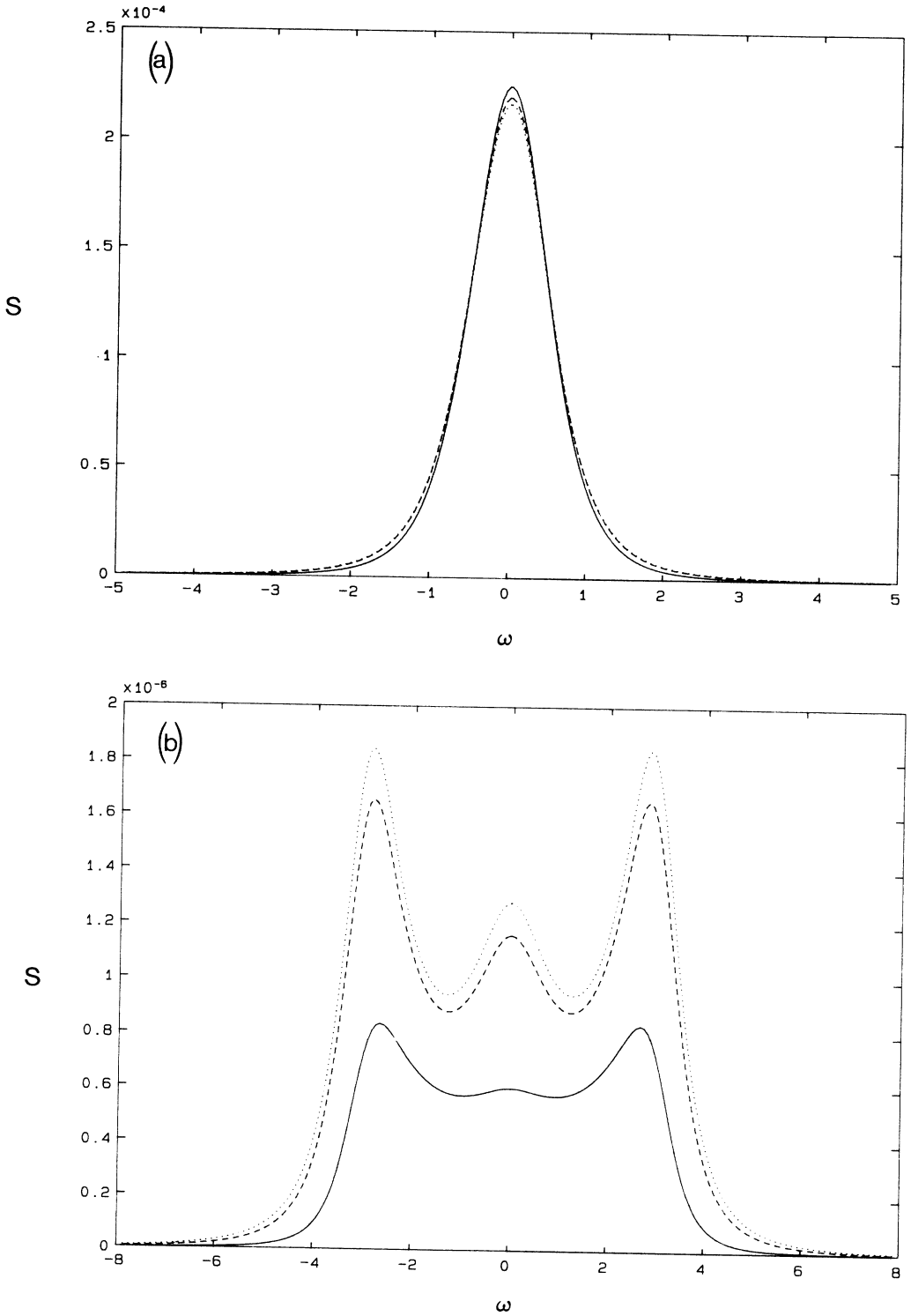

FIG. 5. Power spectra of upper-state population fluctuations $S(\omega)$ in the non-Lorentzian PDM as a function of frequency ω for $b=0.25\kappa$ and $\Omega_0=0.25\kappa$, $\delta=0$ (a); $\Omega_0=0.25\kappa$, $\delta=3\kappa$ (b); $\Omega_0=2.5\kappa$, $\delta=0$ (c), and $\Omega=2.5\kappa$, $\delta=2\kappa$ (d). The different curves correspond to $\beta=2\kappa$ (solid line), $\beta=5.5\kappa$ (dashed line), and $\beta=9\kappa$ (dotted line).

the DRWVPO. Introducing the small quantities $\delta\rho_{10}=\rho_{10}-\bar{\rho}_{10}$, $\delta\rho_{01}=\rho_{01}-\bar{\rho}_{01}$, and $\delta w=w-\bar{w}$ and their Fourier transforms

$$\delta\tilde{x}_j(\nu)=(2\pi)^{-1/2}\int_{-\infty}^{\infty} dt\, e^{-i\nu t}\delta x_j(t)\ , \tag{5.3}$$

we find to lowest order in $(\delta\rho_{10},\delta\rho_{01},\delta w,e)$

$$\tfrac{1}{4}\langle\langle\,\delta\tilde{w}(\omega)\delta\tilde{w}(\omega')\,\rangle\rangle=2S(\omega)\delta(\omega+\omega') \tag{5.4}$$

with

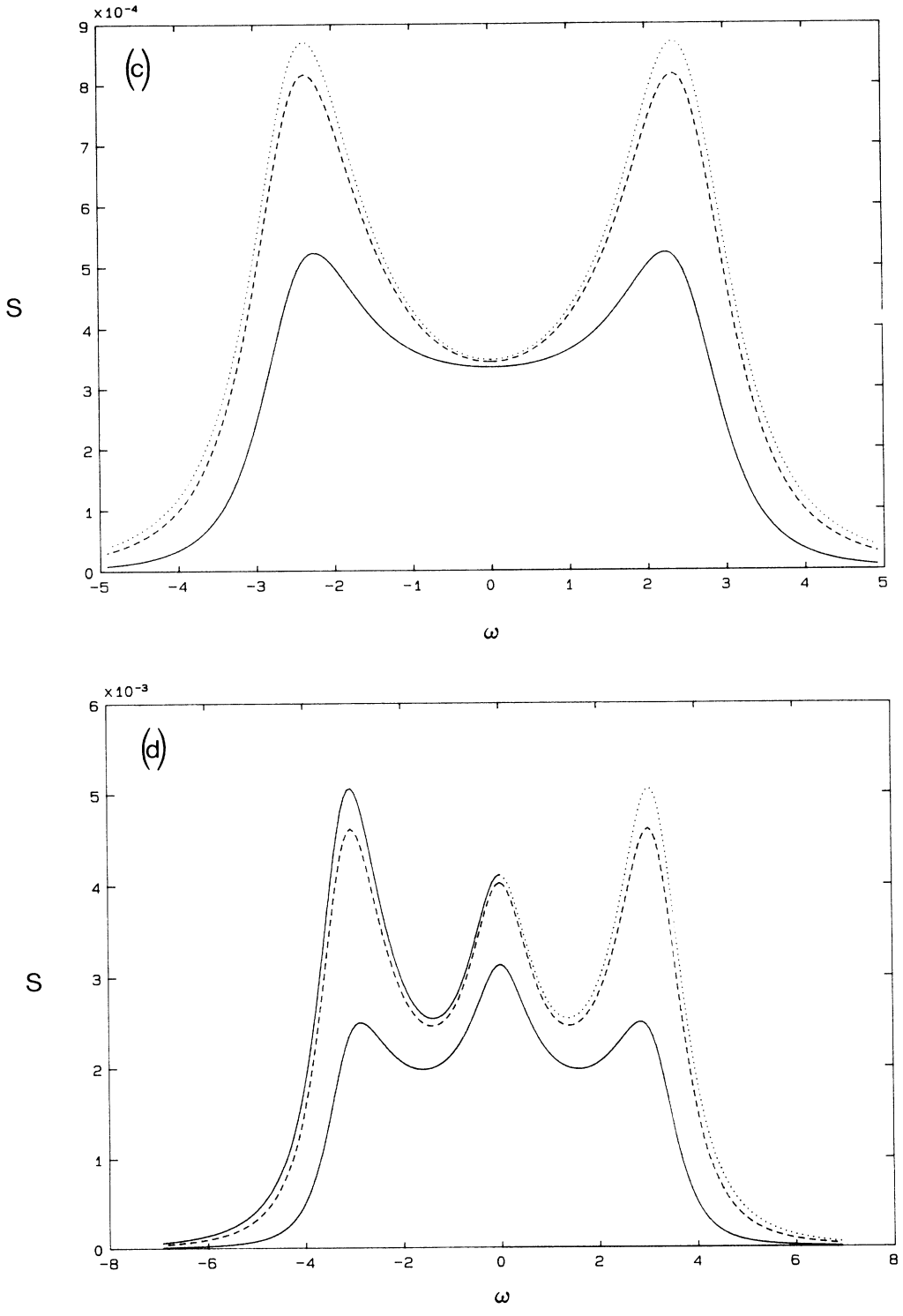

FIG. 5. (*Continued*).

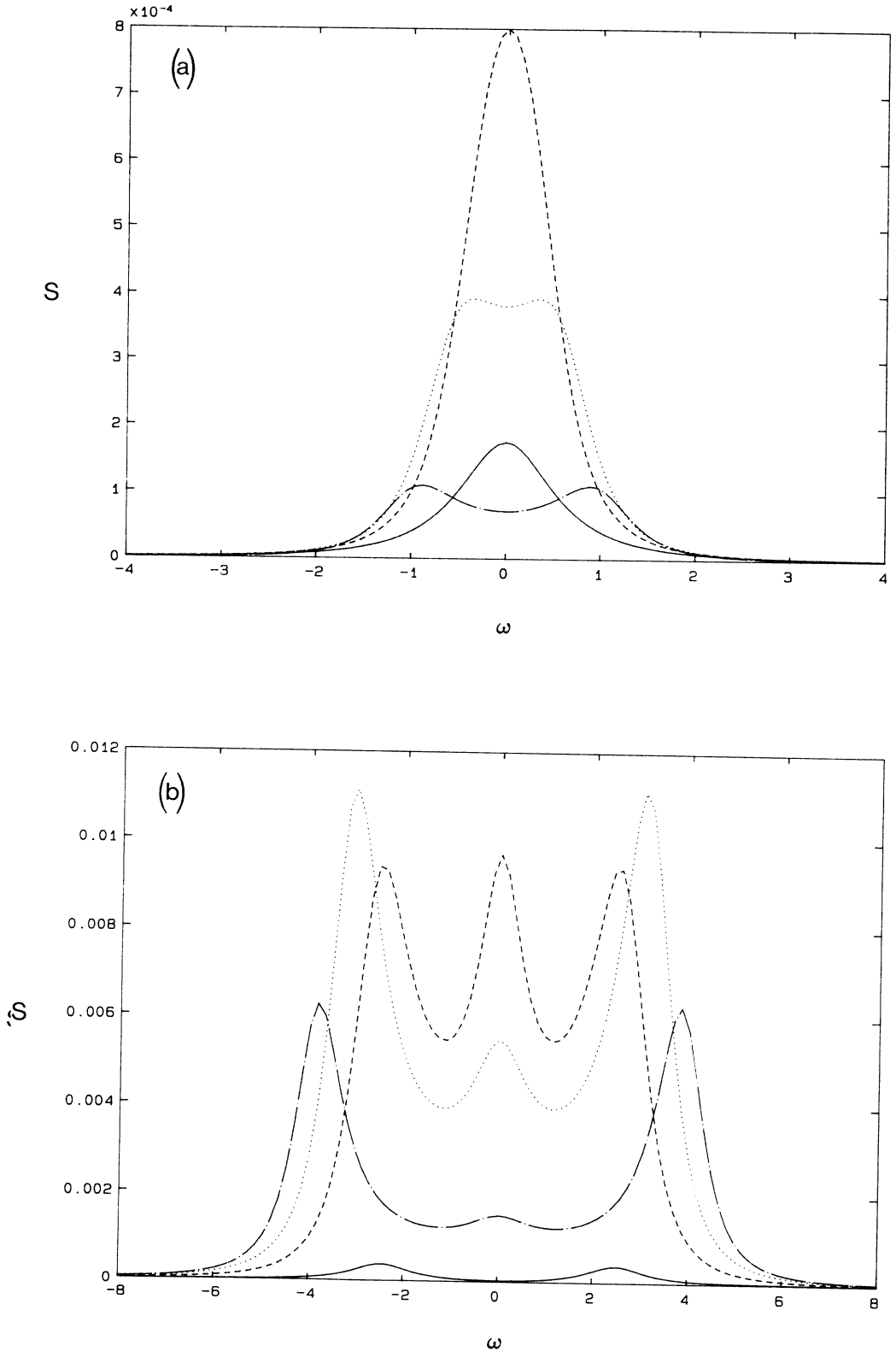

FIG. 6. Power spectra of upper-state population fluctuations $S(\omega)$ for the DRWVPO model as a function of frequency ω for $\Omega_0=0.25\kappa$ (a) and $\Omega_0=0.25\kappa$ (b), with $a_0=4$, $\lambda=3\kappa$, and $\alpha=1$. The laser detunings corresponding to the different curves are $\delta=0$ (solid line), $\delta=0.3\kappa$ (dashed line), $\delta=0.6\kappa$ (dotted line), and $\delta=\kappa$ (dash-dotted line) in (a) and $\delta=0$ (solid line), $\delta=\kappa$ (dashed line), $\delta=2\kappa$ (dotted line), and $\delta=3\kappa$ (dash-dotted line) in (b).

$$S(\omega=is)=\frac{1}{4}\frac{b\Omega_0^4\bar{w}^2}{\left|s+\kappa+\frac{1}{2}\Omega_0^2\frac{\kappa+2s}{k_1}\right|^2}\times\frac{|s+\kappa|^2}{|(s+\frac{1}{2}\kappa)^2+\delta^2|^2|\kappa^2+4\delta^2|}\times\left[\frac{1}{\omega^2+\lambda^2}\left|(\kappa^2+2\kappa s-4\delta^2)-4\alpha\delta\lambda\right|^2+16\delta^2\right], \quad (5.5)$$

where $\bar{w}$ is the stationary mean inversion of the two-level atoms and $k_1=\kappa^2/4+\delta^2+\kappa s+s^2$. In this limit $S(\omega)$ is the sum of two contributions: The first term in the large parentheses arises from the amplitude fluctuations of the input signal and contains also the contribution from the amplitude-noise-induced phase fluctuations. Again the term proportional to $\alpha\delta$ stems from the correlations between amplitude and phase noise and introduces some qualitatively new features in the spectrum. The second term accounts for the usual phase noise and vanishes for zero detuning in this (small-noise) limit (this corresponds to the dip at line center in our previous calculations of the variances). The amplitude-fluctuation-induced noise on the contrary is centered around the atomic resonance $\delta=0$. Both expressions are multiplied by the same function of noise-independent parameters containing resonances at $\omega=0$ and near the Rabi sidebands $\omega\approx\Omega$. Thus for small Rabi frequencies the noise is concentrated around zero frequency $\omega\approx0$. For larger Ω we get an extra resonance at the Rabi frequency. In Figs. 6(a) and 6(b) we show a typical set of such power spectra, by plotting $S(\omega)$ as a function of ω for $a_0=4$, $\lambda=3\kappa$, $\alpha=1$, and four different values of laser detuning $\delta=0$ (solid line), $\delta=0.3\kappa$ (dashed line), $\delta=0.6\kappa$ (dotted line), $\delta=\kappa$ (dash-dotted line), and $\Omega_0=0.25\kappa$ [Fig. 6(a)]. In Fig. 6(b) we have chosen $\Omega_0=3\kappa$ with laser detunings $\delta=0$ (solid line), $\delta=\kappa$ (dashed line), $\delta=2\kappa$ (dotted line), $\delta=3\kappa$ (dash-dotted line), and $\Omega_0=2.5\kappa$. Note that our Eq. (5.4) cannot be compared directly with the predictions of Rzazewski, Stone, and Wilkins[4] who have recently calculated the intensity power spectrum in a weak chaotic field as we assume a strong coherent electric amplitude (around which we linearize).

VI. CONCLUSIONS

In this paper we have presented a theory of laser-noise-induced intensity fluctuations of fluorescence from two-level atoms. The light models considered include the phase-diffusion model with a non-Lorentzian line shape and correlated amplitude-phase fluctuations of a single-mode laser. In general, we find the population variance and its spectrum to be an extremely sensitive probe of the laser light statistics. One of the most interesting effects predicted are pronounced asymmetries in the variances as a function of laser detuning for correlated amplitude-phase noise. The effect of a cutoff of a Lorentzian laser spectrum is to reduce the atomic noise for large frequencies in the power spectrum and for large detunings.

ACKNOWLEDGMENTS

We thank M. Anderson, D. S. Elliott, L. Holberg, R. Jones, R. Ryan, H. Metcalf, S. J. Smith, and C. Wieman for discussions. H.R. and P.Z. acknowledge support by the Fonds zur Förderung der wissenschaftlichen Forschung under Grant Nos. P6008 and P7295. J.C. was supported by the National Science Foundation Grant No. PHY 86-04504.

APPENDIX A: SOLUTION FOR MEAN VALUES, VARIANCES, AND POWER SPECTRA OF STOCHASTIC MULTIPLICATIVE EQUATIONS WITH COLORED NOISE

The purpose of this appendix is to collect some of the more technical steps of solving the multiplicative stochastic Bloch equations (2.10). These equations have the form

$$d\mathbf{u}(t)+[\underline{A}+x(t)\underline{B}]\mathbf{u}(t)dt+\mathbf{I}\,dt=\mathbf{0} \quad (A1)$$

with $\mathbf{u}$ a vector of density matrix elements, $\underline{A}$ and $\underline{B}$ constant matrices, $\mathbf{I}$ a constant vector, and $x(t)$ a colored noise which in our case is an Ornstein-Uhlenbeck process,

$$dx(t)=-bx(t)\,dt+(2b\langle\langle x^2\rangle\rangle)^{1/2}dW(t)\ . \quad (A2)$$

We are interested in calculating averages $\langle\langle u_\mu(t)\rangle\rangle$, $\langle\langle u_\mu(t)u_\nu(t)\rangle\rangle$, and correlation functions $\langle\langle u_\mu(t)u_\nu(t')\rangle\rangle$ with $u_\mu(t)$ solution of a multiplicative stochastic differential equation. The driving field $x(t)$ is a Markov process [Eq. (A2)], thus the conditional probability density $P(x,t|x',t')$ obeys the master equation (Fokker-Planck equation)

$$\frac{\partial}{\partial t}P(x,t|x',t')=L(x)P(x,t|x',t')\ . \quad (A3)$$

The variables $\{\mathbf{u}(t),x(t)\}$ form a Markov process with probability density

$$P(x,u,t|x',u',t')$$

with

$$\frac{\partial}{\partial t}P(x,u,t|x',u',t')=\left[L(x)+\sum_\mu\frac{\partial}{\partial u_\mu}\sum_\nu(A+xB)_{\mu\nu}u_\nu+I_\mu\right]\times P(x,u,t|x',u',t') \quad (A4)$$

and the initial condition

$$P(x,u,t'|x',u',t')=\delta(x-x')\delta(\mathbf{u}-\mathbf{u}')\ .$$

Averages and variances can be found according to

$$\langle\langle u_\mu(t)\rangle\rangle=\int dx\,d\mathbf{u}\,u_\mu P(x,\mathbf{u},t)\equiv\int dx\,u_\mu(x,t) \quad (A5)$$

and

$$\langle\langle u_\mu(t)u_\nu(t)\rangle\rangle = \int dx\, d\mathbf{u}\, u_\mu u_\nu P(x,\mathbf{u},t) \equiv \int dx\, U_{\mu\nu}(x,t) \tag{A6}$$

with $P(x,\mathbf{u},t)$ a solution of (A4). The initial condition for $P(x,\mathbf{u},t)$ is $P(x,\mathbf{u},t_0)=P(x)\delta[\mathbf{u}-\mathbf{u}(t_0)]$ with $P(x)$ the stationary solution of Eq. (A3) and $\mathbf{u}(t_0)$ the (nonstochastic) initial condition of Eq. (A1). The quantities $u_\mu(x,t)$ and $U_{\mu\nu}(x,t)$ are marginal averages. Equations of motion for these marginal averages are easily derived by multiplying Eq. (A4) by u_μ and $u_\mu u_\nu$, respectively, and integrating Eq. (A4) over the variables $\mathbf{u}$. The equation for $u_\mu(x,t)$, for example, reads

$$\frac{\partial}{\partial t}\mathbf{u}(x,t)=L(x)\mathbf{u}(x,t)+[\underline{A}+x(t)\underline{B}]\mathbf{u}(x,t)+\mathbf{I}P(x) \tag{A7}$$

with $u(x,t_0)=u(t_0)P(x)$.

In a similar way the correlation function

$$\langle\langle u_\mu(t)u_\nu(t')\rangle\rangle (t\geq t')$$

can be written as

$$\langle\langle u_\mu(t)u_\nu(t')\rangle\rangle = \int dx\, du \int dx'du'u_\mu P(x,u,t|x',u',t')u'_\nu P(x',u',t') \equiv \int dx\, V_\mu(x,t;\nu)\ , \tag{A8}$$

where $V_\mu(x,t;\nu)$ is the solution of Eq. (A7) with the initial condition

$$V_\mu(x,t';\nu)=\int du\, u_\mu u_\nu P(x,u,t')\equiv U_{\mu\nu}(x,t')\ . \tag{A9}$$

Below we are only interested in the stationary limit where the marginal densities $u_\mu(x,t)$ and $U_{\mu\nu}(x,t)$ become time independent and $V_\mu(x,t;\nu)$ is only a function of the time differences $\tau=t-t'$. As in our previous work (see I and references cited) the equations for the marginal averages can be solved by expansion in the complete set of biorthogonal eigenfunctions of L. Below we summarize some relevant results.

Stationary mean values $\langle\langle\mathbf{u}(t)\rangle\rangle$. As has been shown in Ref. 16, the averages $\mathbf{u}_n(t)$, defined by

$$\mathbf{u}_n(t)=\langle\langle H_n(x(t)/(2\langle\langle x^2\rangle\rangle)^{1/2})\mathbf{u}(t)\rangle\rangle$$

with H_n Hermite polynomials ($n=0,1,\ldots$), obey the equation

$$\left[\frac{d}{dt}+nb+\underline{A}\right]\mathbf{u}_n+(\langle\langle x^2\rangle\rangle/2)^{1/2}\underline{B}\mathbf{u}_{n+1} +(2\langle\langle x^2\rangle\rangle)^{1/2}\underline{B}\mathbf{u}_{n-1}+\mathbf{I}\delta_{n0}=\mathbf{0} \tag{A10}$$

as derived from Eq. (A7). The stationary solution $\langle\langle\mathbf{u}(t)\rangle\rangle=\mathbf{u}_{n=0}(t)$ of Eq. (A10) (assuming that it exists) can be written in terms of a matrix continued fraction

$$\left[\underline{A}-\underline{B}\cfrac{1\langle\langle x^2\rangle\rangle}{1b+A-B\cfrac{2\langle\langle x^2\rangle\rangle}{2b+A-\cdots}B}\underline{B}\right]\langle\langle\mathbf{u}(t)\rangle\rangle+\mathbf{I}+\mathbf{0}\ . \tag{A11}$$

Stationary variances $\langle\langle\mathbf{u}(t)\mathbf{u}(t)^\dagger\rangle\rangle$. In a similar way one can derive equations for the variances of $\mathbf{u}(t)$: rearranging the elements of the covariance matrix in a vector $\mathbf{u}(t)\mathbf{u}(t)^\dagger\rightarrow\mathbf{U}(t)$ we find a system of equations of the type

$$d\mathbf{U}(t)+[\underline{\mathcal{A}}+x(t)\underline{\mathcal{B}}]\mathbf{U}(t)dt+\underline{\mathcal{C}}\mathbf{u}(t)dt=0\ , \tag{A12}$$

with $\underline{\mathcal{A}}$, $\underline{\mathcal{B}}$, and $\underline{\mathcal{C}}$ constant matrices; for the cast of the optical Bloch equations of a two-level system this equation has been explicitly written out in (2.11). Combining $\mathbf{u}$ and $\mathbf{U}$ into a single supervector one obtains an equation which again has the formal structure of Eq. (A10),

$$d\begin{bmatrix}\mathbf{u}\\ \mathbf{U}\end{bmatrix}+\left[\begin{bmatrix}\underline{A} & 0\\ \underline{\mathcal{C}} & \underline{\mathcal{A}}\end{bmatrix}+x(t)\begin{bmatrix}\underline{B} & \underline{0}\\ \underline{0} & \underline{\mathcal{B}}\end{bmatrix}\right]\begin{bmatrix}\mathbf{u}\\ \mathbf{U}\end{bmatrix}dt+\begin{bmatrix}\mathbf{I}\\ \mathbf{0}\end{bmatrix}dt=0\ . \tag{A13}$$

Thus the solution of Eq. (A13) can be obtained in analogy to Eq. (A10) in terms of matrix continued fractions. This provides us with both the stationary mean values $\langle\langle\mathbf{u}(t)\rangle\rangle$ and the second moments $\langle\langle\mathbf{U}(t)\rangle\rangle$.

Spectra. Finally, we turn to the calculation of the spectra defined as the Fourier transform of the stationary correlation function,

$$\underline{S}(\omega)=\mathrm{Re}\left[\int_0^\infty d\tau\, e^{-i\omega\tau}\langle\langle\mathbf{u}(t+\tau),\mathbf{u}(t)^\dagger\rangle\rangle\right] \tag{A14}$$

[compare Eq. (2.4) for the spectrum of the population fluctuations]. Keeping the index ν fixed [$\nu=3$ in Eq. (2.4), corresponding to $w(t)$], we define a vector

$$\mathbf{V}_n(\tau)=\langle\langle H_n(x(\tau)/(2\langle\langle x^2\rangle\rangle)^{1/2})\mathbf{u}(\tau)u_\nu(0)^*\rangle\rangle,$$

which for $\tau\geq 0$ can be shown to obey an equation analogous to (A10),

$$\left[\frac{d}{d\tau}+nb+\underline{A}\right]\mathbf{V}_n(\tau)+(\langle\langle x^2\rangle\rangle/2)^{1/2}\underline{B}\mathbf{V}_{n+1}(\tau) +(2\langle\langle x^2\rangle\rangle)^{1/2}\underline{B}\mathbf{V}_{n-1}(\tau)+\mathbf{I}\delta_{n0}=\mathbf{0}\ . \tag{A15}$$

Taking the Laplace transform of Eq. (A15),

$$\hat{V}(s)=\int_0^\infty d\tau\, e^{-s\tau}V(\tau)\ ,$$

yields

$$(s+nb+\underline{A})\hat{\mathbf{V}}_n(s)+(\langle\langle x^2\rangle\rangle/2)^{1/2}\underline{B}\hat{\mathbf{V}}_{n+1}(s) +(2\langle\langle x^2\rangle\rangle)^{1/2}\underline{B}\hat{\mathbf{V}}_{n-1}(s)+\mathbf{I}\delta_{n0}/s=\mathbf{V}_n(\tau=0)\ . \tag{A16}$$

The μth component of the real part of $\hat{\mathbf{V}}(s=-i\omega)$ gives the spectrum $S_{\mu\nu}(\omega)$. Note that the inhomogeneity $\mathbf{V}_n(\tau=0)$ of this equation at $\tau=0$ is related to the stationary second moments

$$\mathbf{U}_n(t)=\langle\langle H_n[x(\tau)/(2\langle\langle x^2\rangle\rangle)^{1/2}]\mathbf{U}(t)\rangle\rangle\ .$$

To be specific we write this relation as $\mathbf{V}_n(\tau=0)=\underline{D}\mathbf{U}_n$ with $\underline{D}$ a constant matrix. Combining (A16) with Eq. (A13) and the analogous equation for $\mathbf{U}_n$ gives

$$\left[nb + \begin{bmatrix} \underline{A} & \underline{0} & \underline{0} \\ \underline{\mathscr{C}} & \underline{\mathscr{A}} & \underline{0} \\ \underline{0} & -\underline{D} & s+\underline{A} \end{bmatrix} \right] \begin{bmatrix} \mathbf{u}_n \\ \mathbf{U}_n \\ \hat{\mathbf{V}}_n \end{bmatrix} + (\langle\langle x^2 \rangle\rangle/2)^{1/2} \begin{bmatrix} \underline{B} & \underline{0} & \underline{0} \\ \underline{0} & \underline{\mathscr{B}} & \underline{0} \\ \underline{0} & \underline{0} & \underline{B} \end{bmatrix} \left[\begin{bmatrix} \mathbf{u}_{n+1} \\ \mathbf{U}_{n+1} \\ \hat{\mathbf{V}}_{n+1} \end{bmatrix} + 2n \begin{bmatrix} \mathbf{u}_{n-1} \\ \mathbf{U}_{n-1} \\ \hat{\mathbf{V}}_{n-1} \end{bmatrix} \right] + \begin{bmatrix} \mathbf{I} \\ \mathbf{0} \\ \mathbf{I}/s \end{bmatrix} \delta_{n0} = \mathbf{0} \ . \tag{A17}$$

This vector recurrence relation has again a matrix continued-fraction solution which provides us with the atomic mean values, the second moments and the spectrum. Note that the $1/s$ singularity in Eq. (A10) is related to a dc component in the spectrum which is subtracted in the definition of the spectrum.

APPENDIX B: INTENSITY FLUCTUATION SPECTRUM FOR THE PHASE-DIFFUSION MODEL

In this appendix we calculate the spectrum of the atomic upper state population fluctuations for the PDM with Lorentzian line shape. Our starting point is the density matrix equation (2.11) which we write in the form

$$d\mathbf{u}(t) + \underline{A}\mathbf{u}(t)dt + \underline{B}\mathbf{u}(t)\sqrt{2b}\ dW(t) + \mathbf{I}dt = \mathbf{0} \tag{B1}$$

with $dW(t)$ a Wiener increment.[7(c),15] Note Eq. (B1) has to be interpreted as a Stratonovich equation.[7(c),15] The correlation function needed for the spectrum in Eq. (A7) is

$$\langle\langle \mathbf{u}(t+\tau), \mathbf{u}(t)^\dagger \rangle\rangle = e^{(-A+bB^2)\tau} \langle\langle \mathbf{u}(t), \mathbf{u}(t)^\dagger \rangle\rangle \quad (\tau \geq 0, \tau \to \infty) \ , \tag{B2}$$

which gives

$$s(\omega) = \mathrm{Re}[(i\omega + \underline{A} - b\underline{B}^2)^{-1} \langle\langle \mathbf{u}, \mathbf{u}^\dagger \rangle\rangle] \ . \tag{B3}$$

[1]For a review see P. Zoller, in *Multiphoton Processes*, edited by P. Lambropoulos and S. J. Smith (Springer-Verlag, Berlin, 1984); for a fairly recent complete list of references see A. I. Burshtein, A. A. Zharikov, and S. I. Temkin, J. Phys. B **21**, 1907 (1988).

[2]Th. Haslwanter, H. Ritsch, J. Cooper, and P. Zoller, Phys. Rev. A **38**, 5652 (1989), to be denoted as I in this paper.

[3]D. F. Smirnov and I. V. Sokolov, Zh. Eksp. Teor. Fiz. **70**, 2098 (1976) [Sov. Phys.—JETP **43**, 1095 (1976)].

[4]K. Rzazewski, B. Stone, and M. Wilkins, Phys. Rev. A **40**, 2788 (1989); see also K. Wodkiewicz, Sov. J. Quantum Electron. **12**, 656 (1982).

[5]M. W. Hamilton, K. Arnett, S. J. Smith, D. S. Elliott, M. Dziemballa, and P. Zoller, Phys. Rev. A **36**, 178 (1987); D. S. Elliott and S. J. Smith, J. Opt. Soc. Am B **5**, 1927 (1988); K. Arnett, S. J. Smith, R. E. Ryan, T. Bergeman, H. Metcalf, M. W. Hamilton, and J. Ra. Bradenberger, Phys. Rev. A **41**, 2580 (1990).

[6]M. Anderson, D. S. Elliott, R. Jones, and S. J. Smith (unpublished).

[7](a) H. Haug and H. Haken, Z. Phys. **204**, 262 (1967); (b) C. H. Henry, IEEE J. Quantum Electron. **QE-18**, 259 (1982); **QE-19**, 1102 (1983); (c) H. Risken, *The Fokker Planck Equation* (Springer, Berlin, 1984).

[8]Qualitatively such effects have been observed in diode laser experiments by L. Holberg and C. Wieman and co-workers.

[9]R. J. Glauber, Phys. Rev. **130**, 2529 (1963); P. L. Kelly and W. Kliener, Phys. Rev. **136**, 316 (1964).

[10]B. R. Mollow, Phys. Rev. **188**, 1969 (1969).

[11]H. J. Kimble, M. Dagenais, and L. Mandel, Phys. Rev. A **18**, 201 (1978).

[12]Summation over k and l corresponds to averaging over distributions of Doppler shifted atomic eigenfrequencies and the positions of the individual atoms.

[13]Our definition of the off-diagonal density matrix elements differs from Ref. 2 by $\rho_{01}e^{-i\varphi(t)} \to \rho_{01}$.

[14]S. N. Dixit, P. Zoller, and P. Lambropoulos, Phys. Rev. A **18**, 587 (1978).

[15]C. W. Gardiner, *Handbook of Stochastic Methods* (Springer, Berlin, 1983).

[16]P. Zoller, G. Alber, and R. Salvador, Phys. Rev. A **24**, 398 (1981).